Dual-radiolabeled nanoparticle probes for depth-independent in vivo imaging of enzyme activation

Kvar C. L. Black, Mingzhou Zhou, Pinaki Sarder, Maryna Kuchuk, Amal Al-Yasiri, et al.

Kvar C. L. Black, Mingzhou Zhou, Pinaki Sarder, Maryna Kuchuk, Amal Y. Al-Yasiri, Sean P. Gunsten, Kexian Liang, Heather M. Hennkens, Walter J. Akers, Richard Laforest, Steven L. Brody, Cathy S. Cutler, Samuel Achilefu, "Dual-radiolabeled nanoparticle probes for depth-independent in vivo imaging of enzyme activation," Proc. SPIE 10508, Reporters, Markers, Dyes, Nanoparticles, and Molecular Probes for Biomedical Applications X, 1050805 (20 February 2018); doi: 10.1117/12.2301033

SPIE.

Event: SPIE BiOS, 2018, San Francisco, California, United States

Dual-radiolabeled nanoparticle probes for depth-independent *in vivo* imaging of enzyme activation

Kvar C.L. Black[a], Mingzhou Zhou[a], Pinaki Sarder[a], Maryna Kuchuk[b], Amal Y. Al-Yasiri[b], Sean P. Gunsten[c], Kexian Liang[a], Heather M. Hennkens[b], Walter J. Akers[a], Richard Laforest[a], Steven L. Brody[a,c], Cathy S. Cutler[b], Samuel Achilefu[a,d,e,2]

Departments of [a]Radiology, [c]Medicine, [d]Biochemistry & Molecular Biophysics, and [e]Biomedical Engineering, Washington University School of Medicine, St. Louis, Missouri 63110, United States.

[b]University of Missouri, Research Reactor Center, Columbia, Missouri 65211, United States.

ABSTRACT

Quantitative and noninvasive measurement of protease activities has remained an imaging challenge in deep tissues such as the lungs. Here, we designed a dual-radiolabeled probe for reporting the activities of proteases such as matrix metalloproteinases (MMPs) with multispectral single photon emission computed tomography (SPECT) imaging. A gold nanoparticle (NP) was radiolabeled with ^{125}I and ^{111}In and functionalized with an MMP9-cleavable peptide to form a multispectral SPECT imaging contrast agent. In another design, incorporation of ^{199}Au radionuclide into the metal crystal structure of gold NPs provided a superior and stable reference signal in lungs, and ^{111}In was linked to the NP surface via a protease-cleavable substrate, which can serve as an enzyme activity reporter. This work reveals strategies to correlate protease activities with diverse pathologies in a tissue-depth independent manner.

Keywords: bioimaging, nanoparticles, SPECT, MMP, enzyme, in vivo imaging

1. INTRODUCTION

The biochemical functions of enzymes are essential for many normal physiological processes, but their dysregulation contributes to numerous pathologies. Matrix metalloproteinases (MMPs) are a class of enzymes that play a role in disease pathogenesis, including multiple types of cancers, bacterial infection, diabetes, acute lung injury, hypertension, atherosclerosis, and myocardial infarction[1-4]. Therefore, the noninvasive detection of diagnostic enzymes such as MMPs in particular organs has the potential to create a new paradigm in the diagnosis and staging of a range of distinct pathologies. Imaging agents that could accurately report the activity of these enzymes would improve the diagnosis and staging of associated diseases[5, 6]. For optical imaging, these probes generally utilize an enzyme-recognizing and cleavable peptide sequence attached to an emitter and absorber to quench a dye fluorescence *via* an energy transfer mechanism[7]. Upon enzymatic proteolysis of the peptide, fluorescence of the molecular probe increases to allow for *in vitro* and *in vivo* imaging of MMP activity[5, 8, 9]. The activatable optical contrast agents, however, are hampered by significant light attenuation in tissues, which has confined their clinical translatability to a few pathologic conditions.

In contrast, nuclear imaging, which can interrogate enzyme activities noninvasively and quantitatively, cannot utilize a similar quenching phenomenon as fluorescent probes. However, single photon emission computed tomography (SPECT) is capable of resolving multiple reporters based on emitted energy spectrums. Recently, we radiolabeled a single molecule with both ^{111}In and ^{125}I at either end of a caspase-specific cleavable peptide for detecting caspase 3 activity in response to treatment[10]. Small molecule agents have the advantage of rapid clearance, but their pharmacokinetics are not optimal for measuring enzyme activity over long periods.

Nanomaterials hold promise in enabling the synthesis of enzyme activatable contrast agents because of the ease of optimizing their circulation time, biodistribution, and clearance kinetics based on overall size, shape, and surface characteristics[11]. Previously, we incorporated an enzyme-cleavable peptide sequence onto gold NPs that were dually-radiolabeled with ^{111}In and ^{125}I to report the activity of MMP9 in a tumor model by using two-channel SPECT imaging[12].

Reporters, Markers, Dyes, Nanoparticles, and Molecular Probes for Biomedical Applications X, edited by Samuel Achilefu, Ramesh Raghavachari, Proc. of SPIE Vol. 10508, 1050805
 · doi: 10.1117/12.2301033

Here, we explored an alternative strategy that incorporates radiometals directly into metal nanocrystals. Gold in particular offers multiple properties that make it amenable for use in bioimaging, including biocompatibility, ease of synthesis, and well-documented surface functionalization techniques. We designed a novel dual radionuclide activatable SPECT imaging probe for noninvasive measurement of MMP activity. An MMP9-selective cleavable peptide sequence (GPLGVRGK)[13] conjugated to diethylenetriamine N, N, N", N"-tetra acetate-N'-acetic acid (DTPA) for ^{111}In chelation was linked to ^{199}Au-doped gold NPs. Optimization of the imaging scheme allowed us to spectrally differentiate ^{199}Au from ^{111}In, which has the potential to provide quantitative ratiometric imaging of enzyme activity *in vivo*.

2. RESULTS AND DISCUSSION

An aqueous reduction method pioneered by Turkevich[14] was adapted for the synthesis of ^{199}Au doped gold nanocrystals. A few minutes after addition of the sodium citrate reducing agent to the ^{199}Au-containing gold solution, the color transformed gradually from pale yellow to a wine red color, an indication of the formation of gold nanocrystals. The gold nanocrystal suspension demonstrated a localized surface plasmon resonance maximum wavelength of 525 nm, corresponding to NPs of ~15 nm in diameter[15]. Functionalization of the ^{199}Au gold NP with polyethylene glycol (PEG, MW = 5000) was achieved *via* a dibenzocyclooctyne-maleimide (DBCO-maleimide) linker in a stepwise fashion. First, orthogonal reaction of the cysteine thiol from MMP9-cleavable peptide (DTPA-pMMP9: DTPA-Gly-Pro-Leu-Gly-Val-Arg-Gly-Lys-Gly-d-Tyr-Gly-E-Ahx-Cys-NH_2) with the DBCO-maleimide formed a thioether bond with the maleimide, leaving the DBCO functional group to react to an azide on a bifunctional azide-PEG-SH. The ensuing multifunctional PEG conjugate (DTPA-pMMP9-PEG-SH) contained (1) a DTPA moiety for ^{111}In chelation, (2) an MMP9 cleavable peptide, (3) a PEG5000 chain to stabilize the gold NPs in an aqueous medium, and (4) a thiol group for anchorage to the gold surface, yielding the dual-radiolabeled probe (Figure 1).

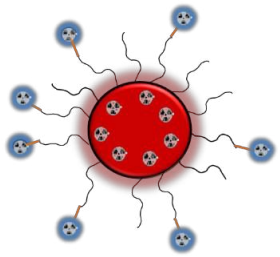

Figure 1. Schematic of dual-radiolabeled SPECT probe with ^{199}Au incorporated directly into a gold nanocrystal and ^{111}In labeled on the end of an MMP cleavable linker.

Aqueous solutions containing the multispectral probe and controls of the individual ^{199}Au and ^{111}In nuclides were imaged with SPECT using two distinct energy windows of acquisition, 159 keV ± 11% (red) and 240 keV ± 60% (blue) (Figure 2*A*). The ^{199}Au control was only detected in the 159 keV channel (608 cps/voxel), retaining the red pseudo-color in the merged image. This corresponded to an intensity efficiency of 2.4 cps/mL/Bq. Since ^{111}In is characterized by γ emissions at both 171 keV and 245 keV, there was the possibility of cross-talk of the 171 keV emission in the 159 keV window. Our analysis showed that signal from ^{111}In was detected in both imaging channels and thus appeared purple in the merged image (3750 cps/voxel in the 159 keV and 3440 cps/voxel in the 240 keV channel). To delineate the concentration of ^{111}In from ^{199}Au, ^{111}In cross-talk was subtracted from the 159 keV channel (see Methods section) to yield 0 cps/voxel in the 159 keV channel and 3440 cps/voxel in the 240 keV channel, corresponding to an efficiency of 45.5 cps/mL/Bq. Gamma signal was detected from the dual-labeled metal nanocrystal in both channels (5430 cps/voxel in the 159 keV channel and 3900 cps/voxel in the 240 keV channel). After ^{111}In cross-talk subtraction from the 159 keV channel, 1130 cps/voxel remained, leading to detection efficiencies of 39.0 cps/mL/Bq for ^{111}In and 4.92 cps/mL/Bq for ^{199}Au. After normalization, the ^{199}Au control appeared red (signal from 159 keV only), the ^{111}In control appeared blue (signal from 240 keV channel only), and the dual-nuclide sample appeared purple (Figure 2*B*).

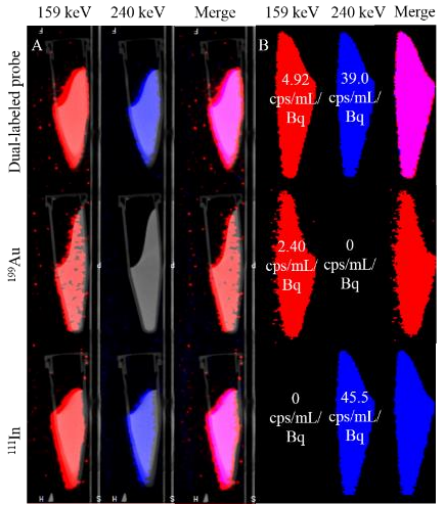

Figure 2. Two channel (159 keV and 240 keV) SPECT imaging of dual-radiolabeled nanocrystal probe phantom (top), ^{199}Au phantom control (middle), and ^{111}In phantom control (bottom) (*A*) before and (*B*) after cross-talk correction. Detection efficiencies are provided for each sample in each energy channel after processing.

To compare the ^{125}I-labeled nanoprobe to the radioactive metal nanocrystal, two probes were synthesized: (1) a similarly pegylated ^{125}I-labeled gold NP used in the recent study[12] and (2) a pegylated radioactive gold nanocrystal, where the nuclide is embedded directly into a metal crystal structure. The two gold NP constructs were injected intratracheally into the lungs of mice and imaged immediately and then 3 and 24 h later (Figure 3). Clear differences in clearance were observed between the two probes. Whereas there was no significant decrease in uptake values of ^{199}Au-doped nanocrystals from the lung even 24 h after injection, a 76% decrease was observed with the ^{125}I-labeled counterparts. These experiments provided clear evidence that a ^{199}Au-doped gold nanocrystal was a viable alternative to the radiochemically unstable ^{125}I-labeled gold NPs, which once nonspecifically detached from the NP clears from the lung.

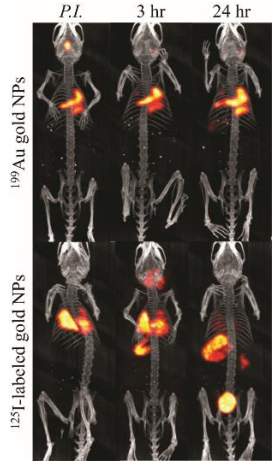

Figure 3. SPECT imaging after intratracheal injection of ^{199}Au-containing gold nanoparticles (top) or ^{125}I-labeled gold nanoparticles (bottom).

We have previously developed a dual radio-labeled probe composed of ^{111}In and ^{125}I, but the ^{125}I-labed gold NPs was unstable *in vivo*[12]. Utilizing a radioactive doping strategy reported previously[16, 17], we achieved *in vivo* radiochemical stability in our current study by incorporating ^{199}Au into the metal nanocrystal structure, which was retained much more significantly in

the lung compared to the unstable ^{125}I (Figure 3). Although the ^{199}Au-doped nanocrystals were designed to serve as a stable source of signal for ratiometric SPECT, the 159 keV emission from ^{199}Au transforms the doped nanocrystals into an imaging agent for a number of applications. For example, SPECT was successfully used to image the accumulation of ^{199}Au gold NPs in the lymph nodes after tail vein injection of the NP in mice. This finding opens the opportunity to use ^{199}Au-doped gold NPs as a SPECT imaging agent for lymph node staging and cancer imaging when appropriately functionalized.

This was the first study to use 2-channel SPECT imaging to distinctly acquire signals from ^{199}Au and ^{111}In simultaneously (Figure 2). With the ^{111}In cross-talk correction in the 159 keV channel, the gamma emission properties of the two isotopes provide an avenue toward two-channel ratiometric imaging capability in mouse lungs. The ^{199}Au/^{111}In ratios could be quantified at every voxel in the 3D SPECT image and represented on an intensity scale. By incorporating enzyme-activatable functionality and avoiding the use of unstable radioiodinated tyrosine *in vivo*, our multispectral SPECT approach is superior to recent studies that uses multimodal imaging to track multiple components of a NP[12, 18].

3. METHODS

Dual-radiolabeled nanocrystal synthesis. ^{199}Au was incorporated into a gold nanocrystal by addition of the nuclide into a gold salt solution, followed by reduction using the Turkevich method. Radio-TLC was performed on each NP batch and confirmed that greater than 96% of ^{199}Au was present in the nanocrystal form, free ^{199}Au was absent in the suspension, and specific activity was 313 MBq/μmol. The pMMP9 was synthesized following a standard Fmoc solid support peptide synthesis procedure. DTPA was conjugated to pMMP9 through amide bond formation. When PEG was covalently bound to the pMMP9 it was conjugated through a DBCO-maleimide linker. The peptide conjugate was anchored to the gold NP surface by a thiol functional group. To form the dual-labeled probe, ^{111}In was chelated to DTPA. Radio TLC confirmed final radiochemical purity to be > 95%; the ^{111}In specific activity was 138 MBq/μmol, corresponding to 68 labeled peptides per NP.

Phantom imaging. Dual SPECT imaging was measured in both the 159 keV and 240 keV channels to capture the γ emission peaks of ^{199}Au and ^{111}In, respectively. Whereas we did not expect cross-talk of the ^{199}Au into the 240 keV window, ^{111}In has two γ emission peaks at 171 keV and 245 keV. The 171 KeV could result in cross-talk contamination in the ^{199}Au channel. As a result, a phantom experiment was performed to define the cross-talk correction factors from the ^{111}In into the ^{199}Au 159 keV window. Three distinct aqueous samples (1 mL each) were imaged: (1) the dual labeled probe described above, diluted to 3.7 MBq ^{111}In and 8.5 MBq ^{199}Au, (2) 9.3 MBq ^{199}Au gold NPs, and (3) 2.8 MBq $^{111}InCl_3$. The following two energy windows were simultaneously acquired to detect ^{111}In and ^{199}Au separately with minimal cross-talk: 240 keV ± 60% was used to image ^{111}In and 159 keV ± 11% was used to image ^{199}Au. The last two samples were used to calculate the nominal detection sensitivity in counts/second/MBq (cps/MBq) for ^{199}Au and ^{111}In and the cross-talk correction factor of ^{111}In into ^{199}Au's 159 keV window in cps/MBq. Samples were imaged with 24 projection scans (60 seconds per scan) in a NanoSPECT/CT (Bioscan, Inc., Washington, D.C.). Images were reconstructed on a matrix of 128 x 128 and 294 frames with 0.300 mm/voxel resolution.

Dual-window SPECT image analysis. The absolute ^{111}In and ^{199}Au activity concentration were determined from the efficiency factors determined from the phantom study and the counts in the 159 keV channel was corrected from the ^{111}In cross-talk contribution as determined from the amount of ^{111}In activity in the 240 keV window. Ratiometric images were then generated from the ratio of absolute ^{111}In and ^{199}Au in each voxel. All computations were performed in MATLAB (MathWorks, Inc., Natick, MA)**.** A ratio image was formed using the estimated ^{199}Au activity concentration in the 159 keV channel (after cross-talk correction) and measured ^{111}In activity concentration in the 240 keV channel. The voxels in which the estimated ^{199}Au activity was computed to be negative or the measured ^{111}In activity was less than 150 cps/voxel were eliminated for the ratio computation to eliminate noisy voxels.

***In vivo* SPECT/CT imaging.** All experiments involving animals were conducted in accordance with protocols approved by the Washington University Animal Studies Committee. C57BL/6J mice were obtained from Jackson Laboratory (Bar Harbor, ME) and housed in a barrier facility. The trachea was surgically exposed, and a 22 G 1" angiocatheter was inserted into the tracheal lumen. NP suspensions comprising 50 μL of ^{125}I or ^{199}Au-labeled gold NP suspension (~10 MBq) were injected intratracheally into mouse lungs in two 25 μL doses 1 min apart. SPECT/CT imaging was performed on the NanoSPECT/CT as described above immediately after injection, as well as 3 and 24 h later.

REFERENCES

[1] J. Rao, "Molecular Mechanisms of Glioma Invasiveness: The Role of Proteases " Nature Reviews Cancer, 3, 489-501 (2003).

[2] A. Pulkoski-Gross, "Historical perspective of matrix metalloproteases.," Front Biosci (Schol Ed). 1(7), 125-149 (2015).

[3] A. T. Hsu, C. D. Barrett, G. M. DeBusk *et al.*, "Kinetics and role of plasma matrix metalloproteinase-9 expression in acute lung injury and the acute respiratory distress syndrome," Shock, 44(2), 128-136 (2015).

[4] A. Yabluchanskiy, Y. Ma, R. Padmanabhan Iyer *et al.*, "Matrix Metalloproteinase-9: Many Shades of Function in Cardiovascular Disease," Physiology, 28, 391-403 (2013).

[5] E. Olson, T. Jiang, T. Aguilera *et al.*, "Activatable cell penetrating peptides linked to nanoparticles as dual probes for in vivo fluorescence and MR imaging of proteases," Proc. Natl. Acad. Sci. U.S.A., 107(9), 4311–4316. (2010).

[6] H. Lee, W. Akers, W. Edwards *et al.*, "Complementary optical and nuclear imaging of caspase-3 activity using combined activatable and radio-labeled multimodality molecular probe," Journal of Biomedical Optics, 14(4), 040507-1 (2009).

[7] Z. Zhang, J. Fan, P. Cheney *et al.*, "Activatable molecular systems using homologous near-infrared fluorescent probes for monitoring enzyme activities in vitro, in cellulo, and in vivo.," Mol. Pharm, 6(2), 416-427 (2009).

[8] T. Aguilera, E. Olson, M. Timmers *et al.*, "Systemic in vivo distribution of activatable cell penetrating peptides is superior to that of cell penetrating peptides," Integr. Biol., 1, 371-381 (2009).

[9] W. Akers, B. Xu, H. Lee *et al.*, "Detection of MMP-2 and MMP-9 activity in vivo with a triple-helical peptide optical probe.," Bioconjug Chem., 23(3), 656-663 (2012).

[10] B. Xu, M. Shokeen, G. Sudlow *et al.*, "Utilizing the Multinuclide Resolving Power of SPECT and Dual Radiolabeled Single Molecules to Assess Treatment Response in Tumors," Mol Imaging Biol, (2015).

[11] E. Blanco, H. Shen, and M. Ferrari, "Principles of nanoparticle design for overcoming biological barriers to drug delivery," Nat Biotechnol, 33, 941-951 (2015).

[12] K. Black, W. Akers, G. Sudlow *et al.*, "Dual-radiolabeled nanoparticle SPECT probes for bioimaging.," Nanoscale, 7(2), 440-444 (2015).

[13] C. Bremer, C.-H. Tung, and R. Weissleder, "In vivo molecular target assessment of matrix metalloproteinase inhibition," Nat Med, 7(6), 743-748 (2001).

[14] J. Turkevich, P. Stevenson, and J. Hillier, "A Study of the Nucleation and Growth Processes in the Synthesis of Colloidal Gold," Discuss. Faraday Soc, 11, 55-75 (1951).

[15] K. Grabar, R. Griffith. Freeman, M. Hommer *et al.*, "Preparation and Characterization of Au Colloid Monolayers," Anal. Chem, 67(4), 735-743 (1995).

[16] Y. Wang, Y. Liu, H. Luehmann *et al.*, "Radioluminescent Gold Nanocages with Controlled Radioactivity for Real-Time in Vivo Imaging," Nano Lett., 13, 581-585 (2013).

[17] Y. Zhao, D. Sultan, L. Detering *et al.*, "Copper-64-Alloyed Gold Nanoparticles for Cancer Imaging: Improved Radiolabel Stability and Diagnostic Accuracy," Angew. Chem. Int. Ed., 53, 156-159 (2014).

[18] J. Llop, P. Jiang, M. Marradi *et al.*, "Visualisation of dual radiolabelled poly(lactide-co-glycolide) nanoparticle degradation in vivo using energy-discriminant SPECT " J. Mater. Chem. B, 3, 6293-6300 (2015).

Acknowledgements

This work was supported in part by grants from the US National Institutes of Health (NCI - U54 CA199092, R01 CA194552, R01 CA152329, P50 CA094056; NHLBI - HHSN268201000046C; NIBIB - R01 EB008111, R01 EB021048), the Department of Defense Breast Cancer Research Program (W81XWH-16-1-0286), and the Alvin J. Siteman Cancer Research Fund (11-FY16-01). Al-Yasiri was supported by the University of Baghdad. We thank the Missouri University Research Reactor for the ^{199}Au synthesis and generously providing the ^{199}Au gold nanocrystal suspensions. We acknowledge Gail Sudlow and LeMoyne Habimana-Griffin for experimental assistance.